Journal of Molecular Structure 1185 (2019) 290–299

Contents lists available at ScienceDirect

Journal of Molecular Structure

journal homepage: http://www.elsevier.com/locate/molstruc

Crystal interactions, computational, spectral and thermal analysis of (*E*)-N'-(thiophen-2-ylmethylene)isonicotinohydrazide as O-N-S-tridentate schiff base ligand

Ismail Warad [a,*], Odey Bsharat [a], Salima Tabti [b], Amel Djedouani [c,d], Mohammed Al-Nuri [a], Nabil Al-Zaqri [e], Karthik Kumara [f], Neartur K. Lokanath [f], Sameer Amereih [g], Ibrahim M. Abu-Reidah [h]

[a] Department of Chemistry, Science College, An-Najah National University, P.O. Box 7, Nablus, Palestine
[b] Laboratory of Electronic Materials and Systems, Faculty of Science and Technology, Mohamed El Bachir University El Anasser, 34000, Bordj Bou Arreridj, Algeria
[c] Superior School of Constantine Assia Djebbar, Constantine 3, 25000, Algeria
[d] Laboratory of Analytical Physicochemistry and Cristallochemistry of Organometallic and Biomolecular Materials, Constantine University 1, 25000, Constantine, Algeria
[e] Department of Chemistry, College of Science, King Saud University, P. O. Box 2455, Riyadh, 11451, Saudi Arabia
[f] Department of Studies in Physics, University of Mysore, Manasagangotri, Mysuru, 570 006, India
[g] Department of Chemistry, Science College, Palestine Technical University, P.O. Box 7, Tulkarm, Palestine
[h] Industrial Chemistry Department, Faculty of Sciences, Arab American University, P.O. Box. 240, 13 Zababdeh, Jenin, Palestine

A R T I C L E I N F O

Article history:
Received 5 June 2018
Received in revised form
24 February 2019
Accepted 26 February 2019
Available online 1 March 2019

Keywords:
Spectral
Crystal structure
O-N-S-Schiff base
DFT-Calculations

A B S T R A C T

The work here focusing on the synthesize of a novel (*E*)-N'-(thiophen-2-ylmethylene)-isonicotinohydrazide as polydentate O-N-S-tridentate Schiff base ligand derived from isonicotinohydrazide and their complexation with $CuCl_2$ center. The structure of O-N-S-ligand was determined by XRD-crystal diffraction and characterized by IR, UV–Vis., CHN-EA, EDX, ^{1}H and ^{13}C-NMR spectroscopy. The DFT/NMR, IR, UV–Vis and optimized structure parameters of the free ligand were matched with their corresponding exp. spectral. The XRD-packing intermolecular has been correlated with the computed Hirshfeld surface analysis (HSA) and MEP-calculation. The Mulliken population and NPA charge analysis, HOMO/LUMO, DOS and global reactivity descriptor quantum parameters (GRD) of the (*E*)-N'-(thiophen-2-ylmethylene)isonicotinohydrazide ligand were also computed under B3LYP/6-311G(d) theory. The coordination of the ligand to Cu(II) centered were monitored by EDX, FT-IR and UV–Visible analysis. The thermal stability of free ligand and its Cu(II)-complex were evaluated by TG-analysis.

1. Introduction

In recent years, many efforts have been carried out to utilize the Schiff bases compounds like isonicotinohydrazide and other hydrazones in industrial applications [1–7]. Poly-chelating ligands designed for metal ions complexation as a serious objective in supramolecular and coordination chemistry now finding global attention [8].

The synthesis of simple chelate Schiff base by the condensation of an aldehyde and isoniazid to produce at an isonicotinohydrazide and their metal complexes have been given great importance in therapeutic chemistry like biological anti-tubercular activity [9–15].

The coordination of metal(II) ions by using Schiff base ligands display a strong selectivity and affinity toward metal(II) centers complexation that have numerous applications like anti-oxidative properties, antitumor activities, photo-physical electronic and attractive properties [10–18].

Copper(II) center exhibited a particularly typical thermodynamic ability for N-S-O-chelate ligand and fast ligand-to-metal binding affinity [16–20].

* Corresponding author. Fax: +970 9234 5982.
E-mail address: warad@najah.edu (I. Warad).

https://doi.org/10.1016/j.molstruc.2019.02.109
0022-2860/

Herein, as novel N-S-O-tridentate chelate Schiff base ligand the (*E*)-N'-(thiophen-2-ylmethylene)-isonicotinohydrazide and its $CuCl_2$ complex were prepared, characterized and HSA/DFT-computed.

2. Experimental

2.1. Measurements

A Jeol-400-NMR spectrometer was served for NMR spectral measurements; the NMR was performed in $CDCl_3$ solvent at RT. UV–Vis. measurements were performed in MeOH solvent using TU- 1901 double-beam spectrophotometer. The FT-IR (MID. 4000-500 cm^{-1}) was recorded in solid state using PerkinElmer Spectrum 1000 FT-IR Spectrometer. MS data was carried out on a 711 A (8 kV) Finnigan. TG spectra were recorded by using a TGA-7 PerkinElmer in 25–900 °C temperature range and with heat rate = 10 °C/min. CHN-analysis was measured using ElementarVarrio EL-analyzer.

2.2. Computational

Gaussian09 software was used to perform all DFT-calculations [21]. Optimizations and frequencies (DFT-IR) of the ligand and its complex were carried out in gaseous state at DFT/B3LYP/6-311G(d), the TD-SCF for the ligand was carried out in MeOH at DFT/B3LYP/6-311G(d), the GIAO/DFT-^{1}H and ^{13}C-NMR for the free ligand were performed in $CDCl_3$ at B3LYP/6-311 + G(2d,p) lever of theory. The CIF file crystallographic data was taken as reference for the calculation when HSA was performed using the CRYSTAL EXPLORER 3.1 [22].

2.3. Crystal data

The X-Ray diffraction data was collected on a Bruker APEX-II D8 diffractometer and goniometre Kappa CCD, equipped with a graphite monochromator using Mo/Ka radiation (λ = 0.71073 Å) at T = 293(2) K. Cell refinement and data reduction were carried out with the APEX2 Software [23]. The structures were solved by direct methods using SHELX97 package [24]. All non-H atoms were refined anisotropically by the full-matrix least-squares method on F2 using SHELXL [25]. The crystal data and structure refinement parameters of the free ligand were illustrated as in Table 1.

Table 1
Crystal data and structure refinement of free ligand.

Empirical formula	C11H9N3OS
Formula weight	231.28
Temperature	293 K
Wavelength	0.71073 Å
Refills, for cell determination	6366
θ range for above	3.06°–27.51°
Crystal system	Triclinic
Space group	*P* − 1
Cell dimensions	$a = 9.2477(10)$Å $b = 10.5120(5)$Å $c = 11.5837(13)$Å $\alpha = 76.820(16)°$ $\beta = 88.034(19)°$ $\gamma = 81.687(19)°$
Volume	1084.9(2) Å^3
Z	4
Density (calculated)	1.416 Mg m^{-3}
Absorption coefficient	0.279 mm^{-1}
F_{000}	480
Crystal size	0.220 × 0.220 × 0.220 mm
θ range for data collection	3.06°–27.51°
Index ranges	$-12 \le h \le 11$ $-13 \le k \le 13$ $-11 \le l \le 15$
Reflections collected	6366
Independent reflections	4830 [$R_{int} = 0.0424$]
Refinement method	Full matrix least-squares on F^2
Data/restraints/ parameters	4830/0/289
Goodness-of-fit on F^2	1.041
Final [$I > 2\sigma(I)$]	$R1 = 0.0551$, w$R2 = 0.1409$
R indices (all data)	$R1 = 0.0775$, w R 2 = 0.1582
Extinction coefficient	CIF-file generated for W-5 P-1 R = 0.06
Largest diff. peak and hole	0.219 and −0.392 *e* Å^{-3}

2.4. Synthesis

2.4.1. Synthesis of (E)-N'-(thiophen-2-ylmethylene) isonicotinohydrazide

A solution of isonicotinohydrazide (1 mmoL) and thiophene-2-carbaldehyde (1.2 mmoL) in EtOH (40 mL) was refluxed for 2 h. Under vacuum the mixture volume was reduced until the product was precipitated (~5 mL). The product was filtered and washed well with *n*-hexane. To obtain single colorless crystal from the product which is good for *X*-ray analysis, the product was re-crystallized at room temperature by slowly evaporation of ethanol solvent from solution.

The white powder product with ~80% yield and m.p = 115–120 °C was collected; molecular formula $C_{11}H_9N_3SO$: Cald. C, 57.13; N, 18.17 and H, 3.92%. Found: C, 57.01; H, 3.83 and N, 18.11%. [M^+] m/z = 231.3 (231.1 theoretical). ^{1}H NMR ($CDCl_3$): ppm) three peaks (1 m and 2d) at δ 7.1–7.8 ppm for thiophene protons, singlet at δ 8.3 ppm for HC=NN-proton, 2d at 8.4–9.1 ppm for pyridine ring protons, singlet at δ 11.9 ppm for proton of amide (see Fig. 4a). ^{13}C-NMR ($CDCl_3$, ppm) 9 Ar's signals from δ 119–165 ppm (Fig. 4b). FT-IR main vibrations, $V_{N\text{-}H} = 3204$ cm^{-1}, $V_{C\text{-}HAr} = 3105$-3020 cm^{-1}, $V_{C\text{-}Hald} = 2880$ cm^{-1}, $V_{C=N}$ = 1615 cm^{-1}, $V_{C=C}$ = 1278 cm^{-1}. UV–Vis. in MeOH: λ_{max} at: 350 nm.

2.4.2. Synthesis of the Cu(II) complex

A solution of ligand (0.41 mmoL) in 10 ml EtOH was mixed to the solution of $CuCl_2\cdot4H_2O$ (0.40 mmol dissolved in 20 ml EtOH under refluxing conditions for 1 h. The change in color confirms the ligand coordination to the metal center. The complex was precipitated from the solution by slowly evaporation of ethanol solvent in a period of 3 days; the solid complex product was filtered and then washed with ethers several times with 75% yield with m.p. 185 °C, conductivity in water: 82 (mS/cm). Molecular formula, $C_{11}H_9Cl_2CuN_3OS$, CHN-EA Cald. C, 36.03; H, 2.75 and N, 11.46%. Found: C, 35.97; H, 2.61 and N, 11.33%, [M^+] m/z = 366.7 (365.8 theoretical). FT-IR (cm^{-1}): $V_{N\text{-}H} = 3180$ cm^{-1}, 3162-2980 ($\nu_{C\text{-}H}$ of Ar's), 1603 ($\nu_{N=C}$), 519 ($\nu_{Cu\text{-}N}$). UV–Vis. in MeOH: λ_{max} at: 350 nm and 440 nm.

3. Results and discussion

3.1. Chemistry

Spectroscopic, elemental analysis and MS provided the structure proof of the (*E*)-N'-(thiophen-2-ylmethylene)-isonicotinohydrazide O-N-S-ligand and its ligand-$CuCl_2$ complex formation as shown in Scheme 1. The desired O-N-S-ligand structure only was proved by XRD-analysis and computed by DFT-calculation for a reason of comparison. Treatment of O-N-S-ligand with one equivalent amount of $CuCl_2\cdot4H_2O$ in methanol led to formation of neutral complex in a very good yield. The desired ligand and its complex were found to be slightly soluble in alcohols, soluble in H_2O and non-soluble in nonpolar solvents i.e. ether.

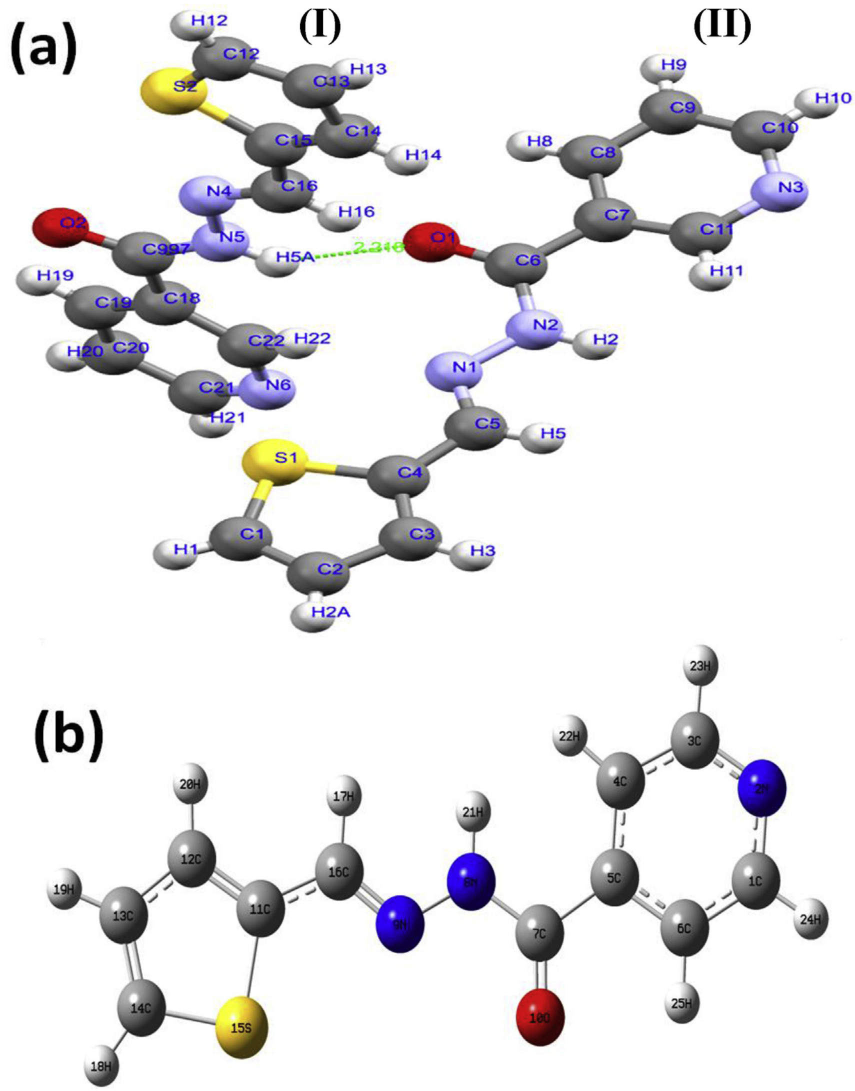

Fig. 1. Ligand structure: (a) ORTEP diagram and (b) optimized ground state geometries at B3LYP/6-311G(d).

3.2. X-ray crystal structure and DFT-optimized structures of the free ligand

The main crystal parameters of the free ligand are reported in Table 2. The ORTEP diagram and B3LYP/6-311G(d) optimized structure of the synthesized ligand are illustrated in Fig. 1.

The N-O-S-ligand crystallized in a triclinic system with P-1 space group (Z = 4) four unit per cell and two ((I) and (II)) independent molecules like Christiane cross-shape interactions. The (I) and (II) molecules are joined *via* strong H-bond of the type N-H ….O=C (2.218 Å) and N-H …. N_{py} (2.174 Å) subsist in a *E*-conformation with regard to the C=N unit but vary in the direction of the thiophene to amide-pyridine rings which minimized the internal-repulsion in both molecule backbone. In both A and B molecules, the C=$N_{imin.}$ bond distance [1.280–1.284 Å] are similar to that reported in (*E*)-4-Bromo-N-(2-chlorobenzylidene)-aniline [26,27]. The N-N bond length [1.380–1.387 Å] is longer compared to similar recorded compounds [28,29]. This elongation may be due to the intermolecular N-H⋯O=C H-bonds that connected A molecule with B molecule. The thiophene/pyidine ring planes dihedral angles C-N-N=C is found to be 170.99° and 174.88°, in A and B, respectively. The C=N-N angle of 115–120° in both A and B molecules reflected the sp^2-hybridization characters of both N atoms which revealed the *E*-isomer as a favored isomer, as seen in Table 2.

The crystallographic data, selected angles and bond lengths structure parameters of (*E*)-N'-(thiophen-2-ylmethylene)-isonicotinohydrazide ligand are listed in Table 2.

The XRD-parameters of the *E*-N'-(thiophen-2-ylmethylene)-isonicotinohydrazide ligand structure like: bond distances and the values of their angles were matched with those derived from the computed DFT/B3LYP/6-311G(d,p) calculation. An excellent matching between calculated and measured results, the correlation between the experimental and calculated bond distances is 0.9966. Similarly, the correlation between the calculated and experimental angles is 0.9922.

3.3. Molecular packing, hirshfeld surface analysis (HSA) and MPE

The molecules are packed in the crystal lattice network as layer–by-layer awarding several short hydrogen bonds (Fig. 2), ten different types of hydrogen-bonds were cited in the crystal-lattice, the main shortest H-bonds are N-H …. N_{py} and N–-H …. .O=C H-

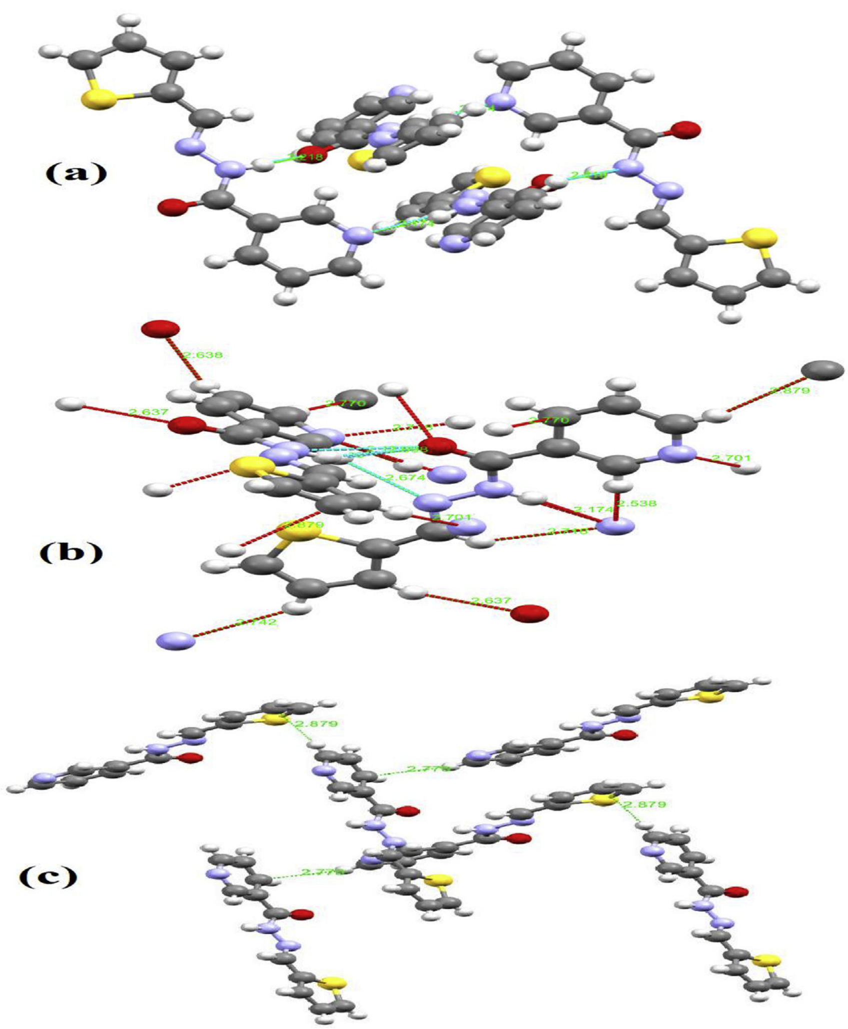

Fig. 2. Molecular packing of free ligand: (a) four molecules connected by N–H–N and N–H–O hydrogen bond types and (b) all intermolecular forces including H-bond and C_{ph}-H … π bonds types.

bond which connect the two molecules together with cross-shape like dimer, these two H-bond play a critical role in strong linking of four molecules in one unit, as seen in Fig. 2a. The other short contacts with different bonds lengths detected in the crystal lattice were illustrated in Table 3 and Fig. 4b. Two weak non-covalent interactions of types C_{ph}-H … π (chelate ring) bonds were also detected per molecule (less than 3 Å) which leads to the formation of supramolecular extra interactions (Fig. 4c and Table 3).

The HSA analysis of the synthesized ligand was performed by using the crystal data file (CIF). Intermolecular contacts were identified as red-spots on the molecule surface [29–33]. Because the desired product contains many heteroatoms like O, S and N in addition to C atoms creating several polar functional groups. Many red-spots were cited on the molecule surface, two big red and two small-spots ones (big spots for strong and small spots for weak interactions) were detected, as in Fig. 3a and b. Interesting, Fig. 3a HSA analysis confirmed the cross-shape like dimer connected perpendicularly through two types of H-bonds, like the XRD analysis. The shortest (big spots) were cited to N–H–N_{py} and N–H–O=C which is strongly consisting with the XRD packing. Moreover, HSA provided the surface also with intermolecular interactions fingerprint (FP) plot as seen in Fig. 3c. Atom-to-atom fingerprint intermolecular forces percentage reflected H–H intermolecular bonds as the largest contributor with 29.6%. The 3 D-FP analyses can document the presence of intermolecular contacts in the following order: H···H > C····H > N····H > O····H > S····H.

A MEP map of (*E*)-N'-(thiophen-2-ylmethylene)-isonicotinohydrazide is very useful in locating the nucleophilic and electrophilic positions in order to figure out the hot interaction positions between molecules in the lattice theoretically [32,33]. The red-color indicated the electron-rich nucleophilic positions, which in the molecule cited to O of carbonyl and N of pyridine (Fig. S1a). The blue color indicated the electrophilic positions (electron-poorness), which in are related only to H atom of the amide functional group. The contour-map lines are used to support MEP result, the electron-rich lines are more around the sulfur, oxygen and nitrogen of imine atoms (Fig. S1b), such seen is consisted with tridentate donation effect of such ligand, as well as the MEP collected result. The presence of red and blue colors together on the surface of the molecule indicated suitable H-bonds interactions since H-donor and acceptor are there. Therefore, N···H····Npy and N···H·····O=C H-bonds were MEP-computed. The crystal molecular-packing and HSA computed analysis reflected the formation of such H-bonds experimentally. Therefore, the MEP theoretical calculation is consistent with experimental analysis.

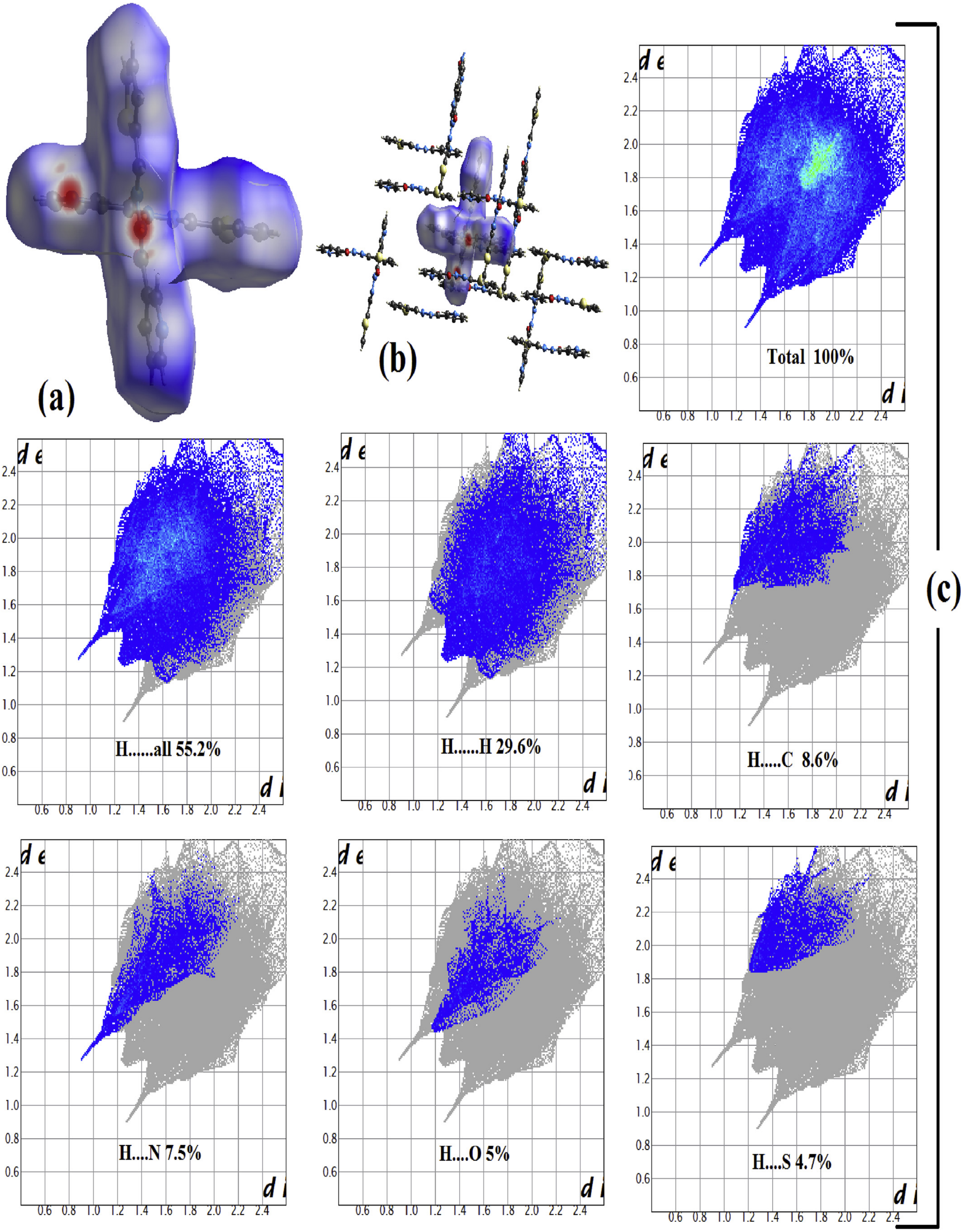

Fig. 3. a) Mapped d_{norm}, b) HSA packing and c) 3D-FP network on the ligand surface.

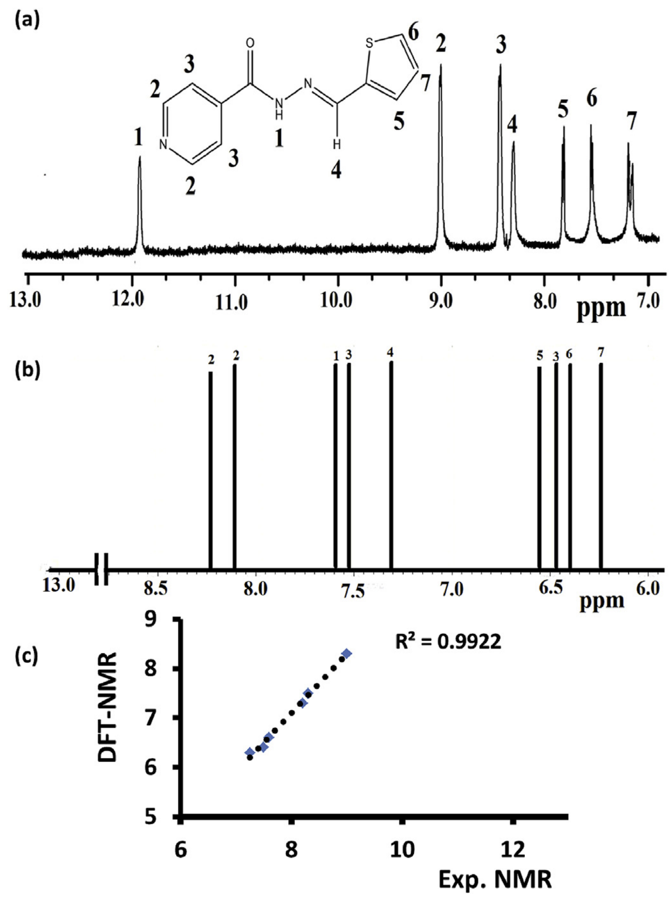

Fig. 4. [1]H-NMR of free ligand in $CDCl_3$: (a) Exp., (b) DFT/B3LYP/6-311 + G(2d,p) GIAO and (c) exp/DFT NMR correlation.

Table 2
XRD-exp. bond lengths (Å) and angles (°) compared to the DFT-calculated ligand structure.

No.	Bonds	Exp. XRD	DFT	No.	Angles (°)	Exp. XRD	DFT
1	S1 C4	1.714	1.749	1	C4 S1 C1	91.4	91.1
2	S1 C1	1.704	1.733	2	C11 N3 C10	116.7	116.8
3	N3 C11	1.340	1.340	3	N2 N1 C5	115.3	116.9
4	N3 C10	1.324	1.337	4	N1 C5 C4	120.7	121.9
5	N1 N2	1.387	1.383	5	N1 N2 C6	118.5	120.8
6	N1 C5	1.28	1.286	6	N2 C6 O1	123.1	123.0
7	N2 C6	1.344	1.358	7	O1 C6 C7	120.3	121.5
8	O1 C6	1.231	1.218	8	S1 C4 C5	121.6	122.3
9	C7 C11	1.385	1.392	9	S1 C4 C3	111.2	110.9
10	C7 C6	1.500	1.511	10	S1 C1 C2	112.8	112.4
11	C7 C8	1.388	1.399				
12	C4 C5	1.448	1.443				
13	C4 C3	1.363	1.360				
14	C1 C2	1.336	1.340				
15	C3 C2	1.42	1.421				
16	C10 C9	1.372	1.379				
17	C8 C9	1.383	1.401				

Table 3
H-bond in (*E*)-N'-(thiophen-2-ylmethylene)-isonicotinohydrazide molecule.

No.	H-bond	Length Å
1	H2···N6	2.174
2	H5A···O1	2.218
3	H20···O1	2.638
4	H3···O2	2.637
5	H11···N6	2.538
6	H5···N6	2.718
7	H2A···N4	2.742
8	H14···N3	2.701
9	H22···N1	2.674
10	H22···O1	2.698
11	H21···C8	2.77
12	H10···C13	2.879

3.4. Mulliken and natural atomic charge population (NPA) analysis

Mulliken atomic charges and NPA play a critical role in quantum-theoretical charge calculations; it gives also helpful information on nucleophilic and electrophilic functional groups that are acting as acceptor/donor atoms [31–33]. B3LYP/6-311G(d) NPA and Mulliken population charge analysis of the ligand data were illustrated in Table S1 and Fig.S2. The study reflected several nucleophilic (e-donor) and electrophilic (e-acceptor) atomic charges. In general, the NPA showed higher atomic-charges compared to Mulliken (Fig.S2). As expected, the Mulliken and NPA reflected the O, N and most of carbon atoms are with nucleophilic characters. The electrophilic sites are localized at: all the hydrogen atoms. The highest electrophilic sites were the amide proton (H21), and carbonyl carbon atom (C7) found to be with positive charge in addition to the sulfur atom of the thiophene ring. The Mulliken and NPA charge result is strongly consistent with MEP, HSA and XRD packing results.

HOMO-LUMO, the density of state (DOS) and Global reactivity descriptors (GRD).

HOMO/LUMO and HOMO-1/LUMO+1 level of energies reflecting the electron donation capacity and degree of electrons acceptance. The HOMO→LUMO orbital shape and energy diagram of the free ligand was illustrated as in Fig.S3a. The density of state (DOS) spectrum has been carried out for the free ligand using GaussSum 3.0 Program, as seen in Fig. S3b. The red and green lines in the computed DOS spectrum indicated all the important molecular orbitals like HOMO, LUMO, HOMO-1 and LUMO+1 energies levels are less than zero, which increased the stability and softness of the ligand, moreover, there are many states ready to be occupied, DOS also reflected the energy gaps (E_g) with 3.898 eV, which is corresponding with the calculated DFT-HOMO/LUMO energy gap (3.974 eV) performed under the same level of theory.

With the help of DFT-calculation, the Global reactivity descriptors (GRD) like: the chemical potential (μ), hardness (η), electronegativity (χ), electrophilicity (ω) and softness (σ) of the

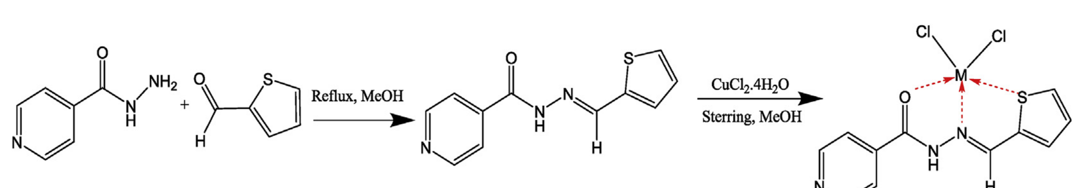

Scheme 1. Preparation of (*E*)-N'-(thiophen-2-ylmethylene)-isonicotinohydrazide and Cu(II) complex.

molecule were predicted by using the reported GRD equations S1-S8.

The GRD data values were collected in Table S2. The molecular orbital energy levels together with their energy gap (3.974 eV) are strongly agreed with the UV-experimental result.

3.5. NMR spectroscopy

The ^{1}H NMR spectrum of (*E*)-N'-(thiophen-2-ylmethylene)-isonicotinohydrazide ligand dissolved in $CDCl_3$ reflected protons with high chemical shifts only, which is consistent with the molecular structure of the ligand (Fig. 4a), δ 7.1–7.8 ppm three peaks (m and 2d) are related to thiophene protons, the broad signal at δ 8.3 ppm is for HC=NN-proton. The pyridine ring protons were appeared as two doublet signals at δ 8.4–9.1 ppm. Proton of amide –NHNC(=O)- is the most acidic one and it appeared as singlet at δ 11.9 ppm.

GIAO ^{1}H NMR DFT/B3LYP/6-311 + G(2d,p) was computed for the free ligand in same exp. solvent ($CDCl_3$) as seen in Fig. 4b, excluding the high shielded amide proton, all the other protons are cited to their expected positions with negligible positive/or negative chemical shifts compared to their corresponding exp.^{1}H NMR chemical shifts. Therefore, an excellent matching with 0.9922 correlation coefficient was recorded by comparing the exp./DFT ^{1}H NMR (Fig. 4c).

^{13}C-NMR spectrum has shown nine carbons-signals in between 119 and 165 ppm, the carbons chemical shifts in (*E*)-N'-(thiophen-2-ylmethylene)-isonicotinohydrazide molecule appeared directly according to their expected positions cited at the spectrum (Fig. 5a). The GIAO ^{13}C NMR DFT/B3LYP/6-311 + G(2d,p) was recorded in $CDCl_3$ and illustrated in Fig. 5b, a good correlation coefficient ~0.9041 was obtained by comparing the exp.^{13}C-NMR to the DFT one (Fig. 5c).

3.6. EDS, MS and elemental analysis

The free ligand and its complex compositions were monitored by EDS-analysis, as seen in Fig. 6. Fig. 6a revealed the free ligand contains: C, O, N and S, whereas the complex contain in addition to C, O, N, S, the Cl and Cu signals atoms, as shown in Fig. 6b, such spectra confirmed the L→M complexation one to one ratio. The absence of un-cited peaks reflected the high purity the prepared material.

The elemental analyses and MS of the desired ligand and ligand-$CuCl_2$ complex are consistent with their proposed molecular formulas.

3.7. Infrared spectra

FT-IR of starting materials, the free ligand and ligand-$CuCl_2$ products were reported as in Fig. 7. The ligand formation during the condensation reaction was monitored by two major changes: 1) the N-H in the isonicotinohydrazide starting material at 3204 cm^{-1} was disappeared by the end of reaction (Fig. 7b). 2) C=O stretching

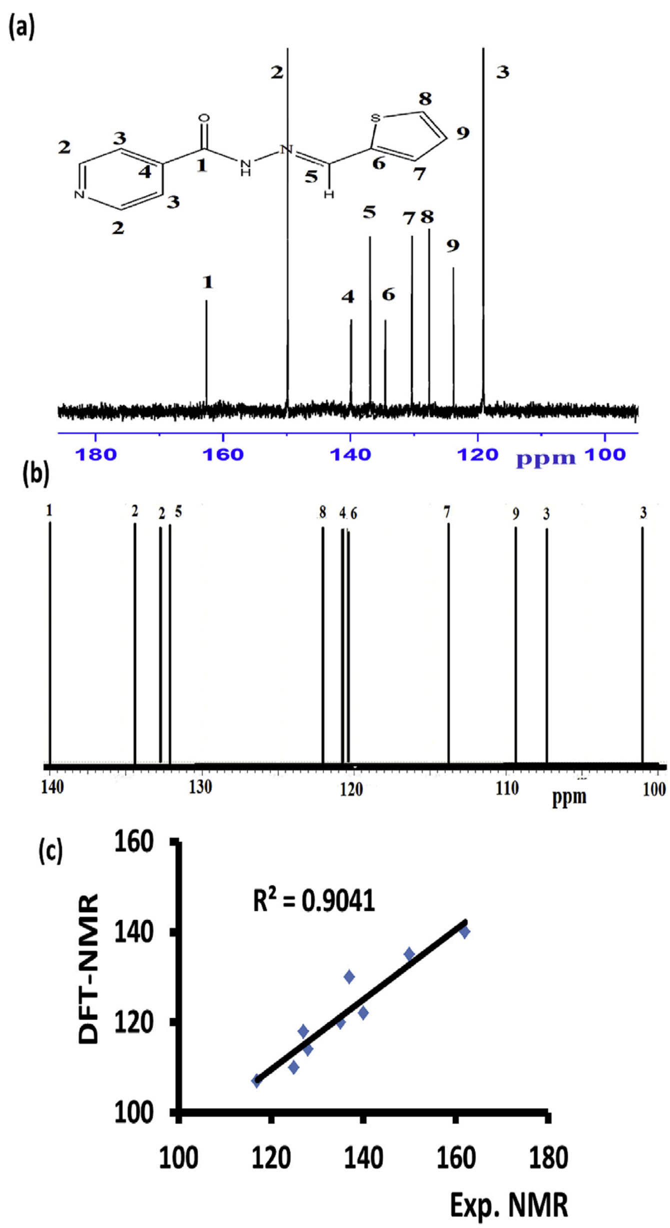

Fig. 5. ^{13}C-NMR of free ligand in $CDCl_3$ (a) Exp. (b) DFT/B3LYP/6-311 + G(2d,p) GIAO and (c) Exp/DFT NMR correlation.

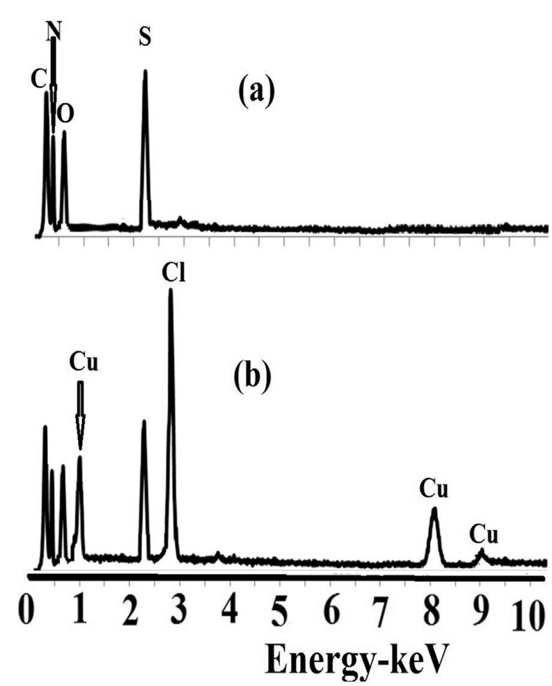

Fig. 6. EDS spectra of: (a) free ligand and (b) ligand-$CuCl_2$.

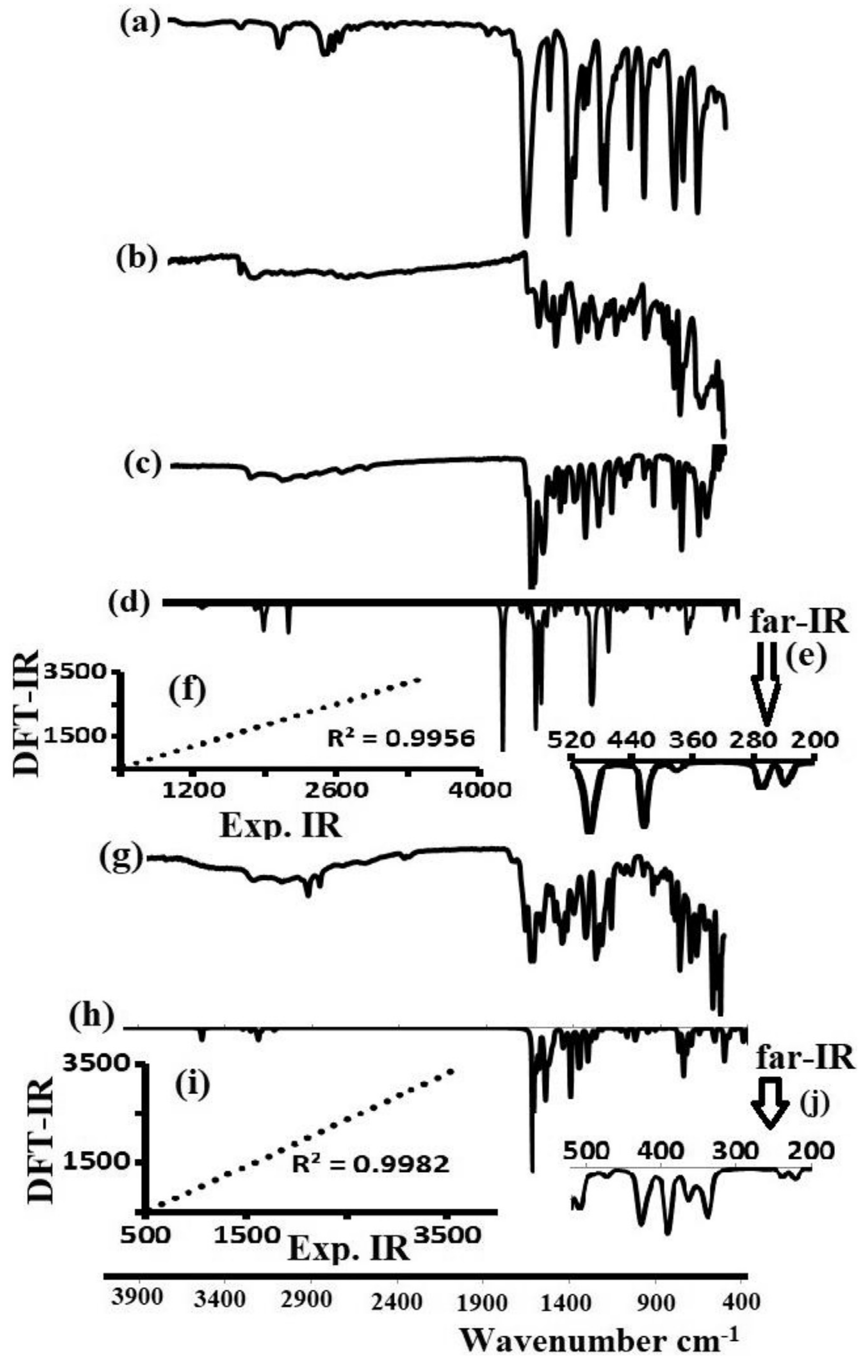

Fig. 7. Exp. FT-IR of (a) thiophene-2-carbaldehyde, (b) isonicotinohydrazide, (c) free ligand, (d) ligand DFT-IR, (f) ligand DFT-far-IR (gaseous state), (e) ligand exp./DFT-IR correlation, (g) solid state of the complex, (h) complex DFT-IR, (i) exp./DFT-IR correlation and (j) complex DFT-far-IR (gaseous state).

vibration in thiophene-2-carbaldehyde starting material at 1665 cm^{-1} (Fig. 7a) was shifted to 1615 cm^{-1} owing to the ligand C=N- formation with $\Delta\nu = 50$ cm^{-1} (Fig. 7c), the free ligand predicted a N-H in-plane deformation with higher intensity than the C=N stretching modes which is consistent with the reported result [34,35]. The main other functional groups stretching vibrations of polar bonds like C-N, C-S, N-N and non-polar bonds like C=C and C-C in the free ligand were sited to their expected area [32–38].

The DFT-IR/B3LYP/6-311G(d) was carried out in gaseous state and illustrated in Fig. 7d, the excellent exp./DFT-IR with its correlation coefficient = 0.9956 reflected a high degree of matching as seen in Fig. 7f, moreover, the 200-500 cm^{-1} DFT -far-IR region was manufactured as seen in Fig. 7e, the N-H out-of-plane deformation is predicted at 422 cm^{-1}, the C_{ph}–H out-of-plane deformation is recorded at 380 cm^{-1}, the C=N out-of-plane deformation is detected at 236 cm^{-1} (Fig. 7e).

In the complex, the $\nu_{(N=C)}$ peak at 1603 cm^{-1} was shifted by 12 cm^{-1} to lower wavenumber compared to the free ligand (1615 cm^{-1}) due to C=N→Cu(II) bond formation. The presence of broad peaks at ~517 cm^{-1} in the vision of the ligand-$CuCl_2$ indicated the N→Cu(II) bonding (Fig. 7g), The gaseous state DFT-IR/B3LYP/6-311G(d) was also illustrated in Fig. 7h, the high correlation coefficient ~ 0.9982 of the plotted DFT/exp.-IR relation reflected an excellent degree of matching (Fig. 7i). In DFT-far–IR region (Fig. 7j),

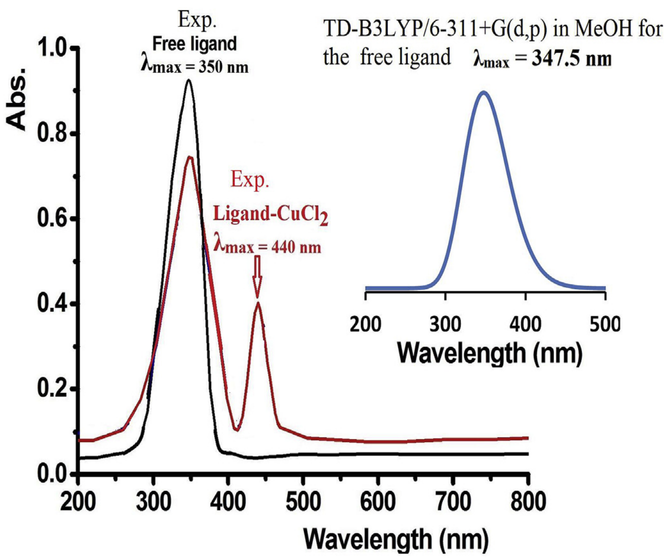

Fig. 8. Exp. UV–Vis. and TD-SCF spectra of the free ligand and its $CuCl_2$ complex (exp.).

Cu-Cl antisymmetric mode is predicted at 361 cm^{-1}, while the symmetric mode at 339 cm^{-1}, the O→Cu(II) and S→Cu(II) coordination bonds vibrations were sited to 505 and 390 cm^{-1}, respectively [32–38].

3.8. UV–vis. spectral analysis

The absorption behavior of the desired ligand and its complex were performed in MeOH at room temperature. The ligand reflected broad peak with $\lambda_{max} = 350$ nm ($\varepsilon = 2.5 \times 10^4\ M^{-1}L^{-1}$) cited to π to π^* electrons transition, as shown in Fig. 8, an excellent matching between exp. UV–Vis. and the computed TD-SCF B3LYP/6-311G(d) in MeOH was recorded, only $\Delta\lambda = 2.5$ nm shift was detected when λ_{max} values was compared. The complex showed two signals; unchanged ligand's peak λ_{max} at 350 nm and ligand to metal charge transfer (LMCT) bands [17] at $\lambda_{max} = 440$ nm ($\varepsilon = 6.4 \times 10^3\ M^{-1}L^{-1}$) for ligand-$CuCl_2$ complex (Fig. 8).

3.9. DFT optimized structure of ligand-$CuCl_2$ complex

The structure of ligand-$CuCl_2$ complex (Fig. 9a) was optimized using DFT/B3LYP/6-311G (d) method, selected bond lengths and angles are cited directly to Fig. 9b. The tridentate N-O-S-ligand coordinated Cu(II) through the N-imine, O-carbonyl and S-thiophene atoms, molding two five-membered chelate rings. The Cl1 and Cl2 atoms are coordinated the center in *cis*-form with Cl-Cu-Cl = 101.4° angle. In general, slightly distorted square-pyramid coordination geometry around the copper center was observed. The Cu-Cl apical distance (2.303 Å) is longer than the Cu-Cl basal distance (2.272 Å), consistent with the probability of finding Jahn-Teller elongated distortion in copper complexes [35–38].

The free ligand structure found to be planar by XRD and this is expected since no sp^3 hybridizations atoms are in its structure, the optimized structure of the Cu-complex reflected the thiophene ring bent away toward the basal Cu-Cl position which lost the ligand planarity (Fig. 9a).

3.10. Thermal stability

TG analysis of the ligand and its $CuCl_2$ complex were performed in an open atmosphere and illustrated in Fig. 10. The ligand

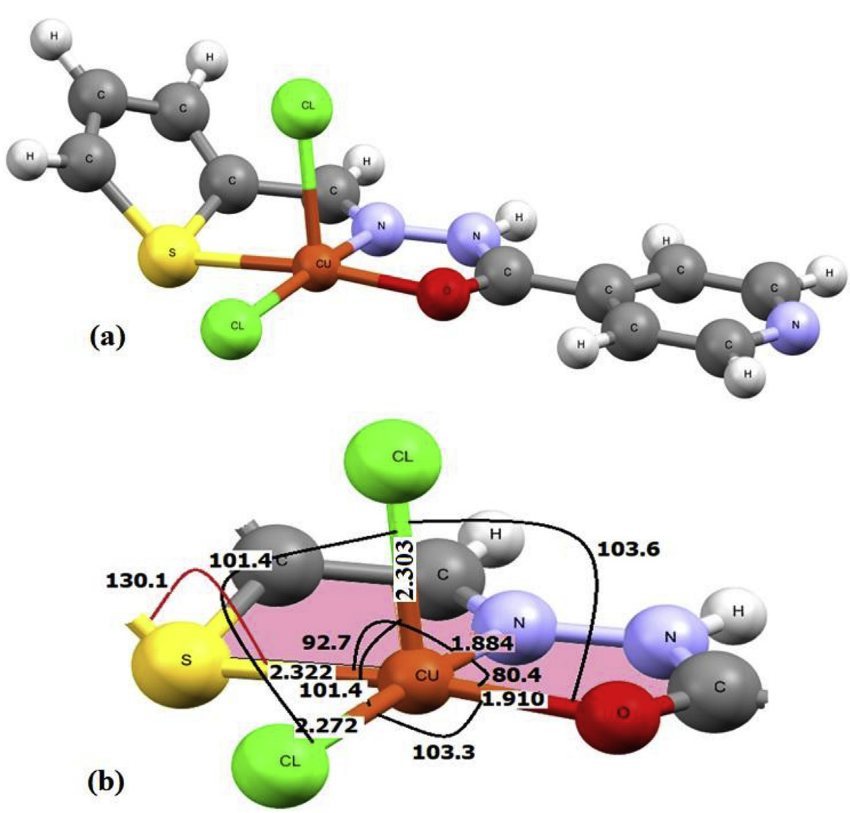

Fig. 9. Optimized structure of Cu(II)-complex.

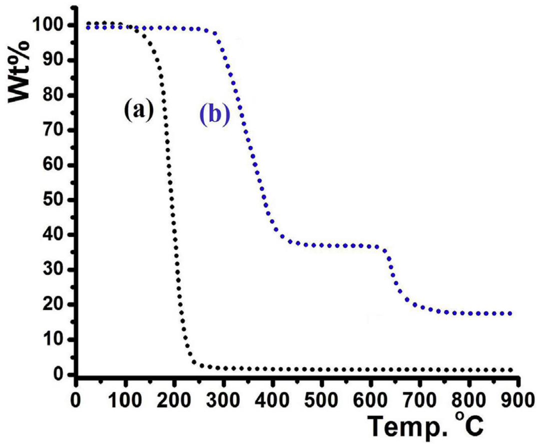

Fig. 10. TG curves: (a) the free ligand and (b) ligand-$CuCl_2$ complex.

decomposed in broad one thermal step at 150–250 °C temperature range (Fig. 10a), meanwhile, the ligand-$CuCl_2$ complex decomposed through two main steps (Fig. 10b). The first step in range of 280–380 °C, attributed to the ligand de-structure from the complex living $CuCl_2$ residue as reflected by a mass loss of ~60%. The second step was decomposing of $CuCl_2 \rightarrow CuO$ (18.3%) as final product in range of 610–740 °C [29].

4. Conclusions

New tridentate O-N-S-Schiff base ligand was synthesized in a good yield; the coordination mode of the desired ligand was evaluated using $CuCl_2$ center. The structure formation of the free ligand and its complex were monitored by FT-IR, EDX, UV–Vis., elemental analysis and MS analyses. The desired ligand structure was proved by X-ray single crystal, CHN-elemental analysis, UV–Vis., FT-IR, EDX, MS, ^{1}H and ^{13}C-NMR. The XRD-structure and molecular packing parameters found to be in a very good matched mode with HSA, Mulliken, NPA charge and MEP computed analysis. The computed ^{1}H, ^{13}C-NMR. IR and TD-SCF UV–Vis. were matched very well compared to their experimental corresponding spectra. Solid state intermolecular forces in the crystal lattice of the free ligand have been clarified experimentally and DFT-theoretically. HOMO/LUMO, DOS and GRD quantum parameters of the ligand were also computed. The TG-thermal behavior of ligand processed with one step thermal decomposing mechanism; meanwhile, the ligand-$CuCl_2$ complex was decomposed *via* two step mechanism.

Acknowledgements

The Project was supported by the Research Center, college of science, King Saud University, Riyadh.

Appendix A. Supplementary data

Supplementary data to this article can be found online at https://doi.org/10.1016/j.molstruc.2019.02.109.

References

[1] A.T. Wright, E.V. Anslyn, Chem. Soc. Rev. 35 (2006) 14–28.
[2] Z. Zhu, J. Zhou, Z. Li, C. Yang, Sens. Actuators, B 208 (2015) 151–158.
[3] L. Prodi, New J. Chem. 29 (2005) 20–31.
[4] T.P. Gazzi, M. Rotta, A.D. Villela, V. Junior, L.K.B. Martinelli, F.M. Sales, E.H. de Sousa, M.M. Campos, L.A. Basso, D.S. Santos, P. Machado, J. Braz. Chem. Soc. 28 (2017) 2028–2037.
[5] A. Zülfikaroglu, H. Bati, N. Dege, J. Mol. Struct. 1162 (2018) 125–139.
[6] Y. Zhou, J. Yoon, Chem. Soc. Rev. 41 (2012) 52–67.
[7] Z. Guo, W. Zhu, H. Tian, Chem. Commun. 48 (2012) 6073–6084.
[8] N. Roy, A. Dutta, P. Mondal, P.C. Paul, T. Sanjoy Singh, J. Lumin. 165 (2015) 167–173.
[9] S. Rollas, Ş.G. Küçükgüzel, Molecules 12 (2007) 1910–1939.
[10] P.F.M. Oliveira, B. Guidetti, A. Chamayou, C. André-Barrès, J. Madacki, J. Kordulákova, G. Mori, B.S. Orena, L.R. Chiarelli, M.R. Pasca, C. Lherbet, C. Carayon, S. Massou, M. Baron, M. Baltas, Molecules 22 (2017) 1457–1469.
[11] H. Zafar, M. Hayat, S. Saied, Momin Khan, U. Salar, R. Malik, M. Choudhary, Khalid Mohammed Khan, Bioorg. Med. Chem. 25 (2017) 2351–2371.
[12] K. Hruskova, P. Kovarikova, P. Bendova, P. Haskova, E. Mackova, J. Stariat, A. Vavrova, K. Vavrova, T. Simunek, Chem. Res. Toxicol. 24 (2011) 290–302.
[13] V.C. Da Silveira, J.S. Luz, C.C. Oliveira, I. Graziani, M.R. Ciriolo, A.M. Ferreira, J. Inorg. Biochem. 102 (2008) 1090–1103.
[14] K. Hruková, E. Potůčková, T. Hergeselová, L. Liptáková, P. Hašková, P. Mingas, P. Kovaříková, Š.,T. imůnek, K. Vávrová, Eur. J. Med. Chem. 120 (2016) 97–110.
[15] B.R. Stern, J. Toxicol. Environ. Health A. 73 (2010) 114–127.
[16] D. Aggoun, A. Ourarri, R. Ruiz-Roses, E. Moralon, Spectrochim. Acta A. 184 (2017) 299–307.
[17] S. Tabti, A. Djedouani, D. Aggoun, I. Warad, S. Rahmouni, S. Romdhane, H. Fouzi, J. Mol. Struct. 1155 (2018) 11–20.
[18] I. Warad, M. Abdoh, A. Al Ali, N. Shivalingegowda, K. Kumara, A. Zarrouk, N.K. Lokanath, J. Mol. Struct. 1154 (2018) 619–625.
[19] D. Bouknana, B. Hammouti, B. Salghi, A. Zarrouk, I. Warad, J. Mater. Environ. Sci. 5 (2014) 1039–1058.
[20] T.B. Hadda, M. Ali, V. Masand, S. Gharby, T. Fergoug, I. Warad, Med. Chem. Res. 22 (2013) 1438–1449.
[21] M.J. Frisch, G.W. Trucks, et al., Gaussian 09, Gaussian Inc., Wallingford CT, 2009.
[22] S.K. Wolff, D.J. Grimwood, J.J. McKinnon, D. Jayatilaka, M.A. Spackman, Crystal Explorer 2.1, University of Western Australia, Perth, 2007.
[23] A.P.E.X.2 Bruker, SAINT and SADABS, Brucker AXS Inc., Madison, WI, USA, 2012.
[24] G. Sheldrick, SHELXL-97, Universitat Geottingen, Geottingen, Germany, 1999.
[25] R. Ennington, T. Keith, J. Millam, Semichem Inc. Shawnee Mission KS, GaussView, Version, 5, 2009.
[26] C. Wang, Acta Crystallogr. E67 (2011) 2204–2206.
[27] G. Alpaslan, O. Özdamar, M. Odabaşoğlu, C. Ersanlı, C. Büyükgüngör, A. Erdönmez, Acta Crystallogr. E61 (2005) 2428–2430.
[28] G. Alpaslan, O. Özdamar, M. Odabaşoğlu, C.C. Ersanlı, O. Büyükgüngör, A. Erdönmez, Acta Crystallogr. E61 (2005) 3442–3444.
[29] I. Warad, Y. Al-Demeri, M. Al-Nuri, S. Shahwan, M. Abdoh, S. Naveen, N.K. Lokanath, M.S. Mubarak, T.B. Hadda, Y.N. Mabkhot, J. Mol. Struct. 1142 (2017) 217–225.
[30] F.A. Saleemh, S. Musameh, A. Sawafta, P. Brandao, C.J. Tavares, S. Ferdov, A. Barakat, A. Al Ali, M. Al-Noaimi, I. Warad, Arab. J. Chem. 10 (2017) 845–854.
[31] M.A. Spackman, D. Jayatilaka, Cryst. Engg. Comm. 11 (2009) 19–32.
[32] M.R. Aouad, M. Messali, N. Rezki, N. Al-Zaqri, I. Warad, J. Mol. Liq. 264 (2018) 621–629.
[33] M.R. Aouad, M. Messali, N. Rezki, M.A. Said, D. Lentz, L. Zubaydi, I. Warad, J. Mol. Struct. 1180 (2019) 455–461.
[34] M.V. Castillo, J.L. Pergomet, G.A. Carnavale, L. Davies, J. Zinczuk, S.A. Brandán, F.T.I.R. FT-Raman, J. Mol. Struct. 1142 (2017) 18–27.
[35] A.E. Ledesma, C. Contreras, J. Svoboda, A. Vektariane, S.A. Brandán, J. Mol. Struct. 967 (2010) 159–165.
[36] B. Rajasekhar, N. Bodavarapu, M. Sridevi, G. Thamizhselvi, K. RizhaNazar, R. Padmanaban, T. Swu, J. Mol. Struct. 1156 (2018) 690–699.
[37] C. Huerta-Aguilar, P. Thangarasu, J.G. Mora, J. Mol. Struct. 1157 (2018) 660–671.
[38] I. Warad, F.F. Awwadi, B. Abd Al-Ghani, A. Sawafta, N. Shivalingegowda, N.K. Lokanath, M.S. Mubarak, T. Ben Hadda, A. Zarrouk, F. Al-Rimawi, A. Bani Odeh, S.A. Barghouthi, Ultrason. Sonochem. 48 (2018) 1–10.